Research article

Alkali activation of compacted termite mound soil for eco-friendly construction materials

Assia Aboubakar Mahamat [a,*], Ifeyinwa Ijeoma Obianyo [a], Blasuis Ngayakamo [a], Numfor Linda Bih [a], Olugbenga Ayeni [a,d], Salifu T. Azeko [b], Holmer Savastano Jr. [c]

[a] Department of Materials Science and Engineering, African University of Science and Technology, Abuja, Federal Capital Territory, Nigeria
[b] Department of Mechanical Engineering, Tamale Technical University, Tamale, Ghana
[c] Department of Biosystems Engineering, University of Sao Paulo, Pirassununga, Sao Paulo, Brazil
[d] Department of Building, Faculty of Environmental Design, Ahmadu Bello University, Zaria, Nigeria

ARTICLE INFO

ABSTRACT

This investigation prospects the feasibility of optimizing the mechanical behavior and dimensional stability of termite's mound soil through alkaline activation. The raw aluminosilicate (termites' soil) was used without any pre-thermal treatment and natural occurring potash was used as the alkaline activator. Different activation level and different initial curing temperature were adopted to examine the effect of the initial temperature and the activator concentration on the Alkali Activated Termite Soil (AATS). Similarly, Scanning Electron Microscopy (SEM)/Energy Dispersive X-ray Spectroscopy (EDS), X-ray Diffraction (XRD) and Fourier Transform Infra-Red Spectroscopy (FTIR) were conducted to characterize the microstructure, to determine the crystallinity of the constituents and to identify the functional groups present within the specimens. These characterizations were carried out on the specimens at 15 days after their moulding. The compressive strength was determined for 7, 15 and 90 days to illuminate the fundamental of the optimization process. Results showed that the optimal initial curing temperature was 60°C for the oven-dry regime at 3wt% activator with compressive strength of 2.56, 4.38 and 7.79 MPa at 7, 15 and 90 days respectively. From the mechanical performances results, the alkali stabilized termite's soil can be used as masonry elements predominantly submitted to compression. The repercussions of the results are analyzed for potential applications of the Alkaline Activation techniques as an environmental-friendly approach to obtain renewable and sustainable building materials at low cost with low energy consumption henceforth replicable in most of the regions.

1. Introduction

Globally, the building and construction industry plays a major role to the accumulation of greenhouse gas emissions. This industry alone produces approximatively 30% of greenhouse gas emissions worldwide. It accounts for 40% of worldwide energy, 25% of worldwide water and 40% of worldwide resources (UNEP (2014)). Cement is the most conventional used material in the construction industry. In 2019, cement production was approximately 4.2 billion tons per year making it the second-high volume commodity after water [1]. The Greenhouse gas emissions related to cement are largely from the energy consumption during the manufacturing of the raw materials to building's demolition. Cement utilization is extremely connected with depletion of mineral reserves particularly in regions where cement consumption rate is higher than the natural resources available.

Financial constraints, available resources would be the primary factors controlling a construction material's choice. On that account, green building technologies have overtaken the construction industry in the last decades. These green building technologies consist of the implementation of constructing using environmental-friendly processes in all the parts of the building's life [1]. The advantages of green buildings are environmental-friendly, natural resources and energy efficiency [2], low cost, and sustainability as a result increasing residents productivity [3]. Among the green buildings' materials, earth-based materials are the most commonly used historically. The use of earth-based materials in construction application is as old as mankind itself. Earth-based materials can be divided into minerals, rocks, soil and water. They constitute the

raw material obtained on the earth crust. Nevertheless, not all earth-based materials can be used in construction; their utilization as building materials depends principally on their properties. Termites Mounds Soil is the soil obtained from the termite's hill. During the construction of their nest (hill), termites use their salivary secretions and faeces to modify the surrounding soil through biological processes [4] making it a stronger material that can resist erosions over decades. But Kandasami et Al. found that the Atterberg limits (which are commonly used as signatures of clay mineralogy were not different between the termite's mound soil and the surrounding soil) [4] confirming that termites are not effecting any changes in clay mineralogy of the mound soils, contrary to what has been suggested by some researchers [5].

Termite's Mounds are spread throughout the tropics. Pomeroy investigated the abundance of termite mounds in Uganda [6], while in Nigeria, Ackerman studied their spread and effect on the environment [7, 8] and Jean-Pierre B. studied the spatial distribution of termite's mounds soil in a protected environment in ivory coast [9]. The use of the termite's mounds soil as a construction material is empirical and traditional without clear scientific explanation behind its usage, despite many studies carried on the termite's mounds soil a clear understanding has not come forth. Elinwa investigated the pozzolanic potential of the calcined termites' mounds, the addition of the calcined termites' mounds clay significantly advanced the initial and final setting times thus they classify it as an accelerator [10]. It's noteworthy that from their chemical analysis the calcined termites' mounds were predominantly composed of SiO_2, Al_2O_3, Fe_2O_3 with a near-neutral pH (7.5). In the termite's mounds, temperature and gases appear to be regulated therefore the interest of engineering these soil structures for sustainable and green construction. Investigations carried by [11] on termite's mounds clay showed that the use of water-repellent chemical contributed to reducing the water absorption level. In their investigation they used hydrated lime and silane/siloxane as additive to the Termites mounds clay. The inclusion of water-repellent admixture prevented thickness swelling of the samples and produced reduction in voids causing high compressive strength. While Kandasami examined the physical attributes of the termite's mound to analyze the internal network of the galleries and tunnels. They concluded that the porosity of the termite mound soil varied with the porosity increasing from the base to the top of the termite's mound, proving the effect of erosion on the top region of the mound [4]. Those applications of the termite mound soil from the literature show the benefits of termite mound soil as a construction material; the main advantage is its natural pozzolanic features. The usage of termite's mounds soil in construction is restricted due to its sensibility for water; the problem of elevated moisture contents remains unresolved. Thus, Kandasami suggests that termite mounds soil can be restricted only to drier climatic zones or those where rainfall spells are not prolonged. The product can waterproof and join the soil components. Gandia studied the physical, mechanical and thermal properties of adobe stabilized with the "synthetic termite saliva" [12]. The incorporation of the "synthetic termite saliva" into the soil, presented greater clay mineral particle cohesion and high hydrophobicity. But the use of "synthetic termite saliva" negatively interfered with compressive strength. Hence, stabilization is a treatment used to improve the durability, strength of soils, also properties such as reduced plasticity and swelling potential are expected to be improved after the stabilisation [13]. There are many types of stabilizations, from mechanical to chemical. One type of chemical stabilisation is the Alkali activation. Alkali activated material encompasses any binder derived from the reaction of an alkali source with an aluminosilicate solid precursor [14] forming a solid material comparable to hardened Portland cement [15]. The use of an alkaline activating solution does improve the soils stability and reintroduce Greenhouse. Alkali activation technology offers the opportunity to utilize locally natural occurring raw materials as precursor (Termites mounds soil) and activators (potash) with performances as good as cement, the termites mound used is an aluminosilicate-rich precursor subsequently it's desirable to use an alkali hydroxides source [15] subsequently the choice of

potassium hydroxides. For Alkali Activated Materials (AAM), the gas emission was calculated to be lower than cement by 80 to 30% [16], the depletion of natural reserves is less because the Alkali activation technology allows to use waste ashes [17] and slags [18] into valuable materials by reducing heavy metals emission to the environment. Alkali activated materials are resistance to high temperature and fire, resistance to acid and chemical attack, volumetric stability after hardening, low thermal conductivity, low permeability and low cost [14]. The alkaline nature of the stabilizer affects greatly the pH of the soil by increasing it. But, in some cases the alkalinity will start decreasing at the late curing ages because of the decrease in calcium ions as the hydration reaction progresses. That consumption of alkalinity indicates the occurrence of bonds formation and strengthening of soils [13]. The degradation of Alkali activated materials is much lower than the modern cement degradation as demonstrated by the Roman structures' resistance to degradation over the time.

Alkali activation has been proved to be a very friendly technique for mechanical improvement of aluminosilicates. Subsequently, the difference of this study from previous literature is to link the microstructure to the macrostructural responses. To achieve that, a better understanding of the alkali activation's effect on the termite's soil is required. It's foreseen that the alkali activation will greatly affect the mechanical behavior and dimensional stability of the termite's soil as a building material. This technique can reduce the CO_2 emission related with conventional building materials and the technique is easily practicable everywhere without very high energy consumption required thus breaking down the cost of sustainable housing.

The development of green, renewable and sustainable materials from termite mound soil through alkaline activation by the utilization of natural potash is aimed in this investigation. The derived objectives will increase standard housing accessibility in regions where the termite soil is abundant and doesn't represents any economic value (specifically in the sub-Saharan region).

2. Experimental procedure

2.1. Materials

The termite mound soil was obtained from deserted and inhabited mounds in Abuja, Nigeria. The soil was crushed manually and sieved prior to its usage as precursor during the samples moulding. The particle size distribution was performed by mechanical sieving and sedimentation (showing that the termite soil contained 50% of soil) in accordance with the BS 1377:2. The moisture content, Atterberg limits and specific gravity were performed on the soil. Table 1 shows the different properties of the soil. Electron Dispersive Spectroscopy EDX was used to determine the elemental composition of the termite mound.

Potassium alum or potash was obtained from, FCT-Abuja, Nigeria. The potash was obtained in the form of coarse grains with a whitish color. This was ground to powder in a laboratory mechanical grinder. Its chemical composition was determined with EDX analysis the results showed that this potash is from the potassium sulfate group. The KOH was used due to its availability, its low cost, environmental-friendliness and performances. Thus, it was used in its natural occurrence as potash. Additionally, previous study showed that the use of NaOH as a chemical activating agent in natural pozzolan delayed the formation of and resulted in greater deformations for the samples [19]. It's noteworthy to recall that the TMS has been previously classified as natural pozzolana

The mixtures were prepared with 1, 3 and 5wt% of the activator and 15wt% of water. The precursor and activator were dry mixed in a laboratory mixer for 5 min before adding water at room temperature ($27°C$) and mixed for additional 5 min before pouring the paste into moulds of dimensions $50 \times 50 \times 50$mm. The alkali activated termites' soil (AATS) was produced by one-part mix technique because of the similarity of the process in manufacturing earthen masonry units. Compaction technique was adopted for the production of the specimens based on results ob-

Table 1. Termite's soil physical and chemical characteristics.

Chemical composition	Mineral content	Particle size distribution	Atterberg limits	Specific gravity	Bulk density
SiO_2 51.26%	Quartz	Clay 48%	Plastic Limit 30.17%	2.61	1.49 g/cm^3
Al_2O_3 23.89%	Kaolin	Sand 34%	Liquid Limit 17.9%		
Fe_2O_3 21.80%		Silt 18%	Plasticity Index 12.2%		
Others 3.05%			Linear Shrinkage 6.5%		

tained in Figure 1. Studies have shown that the moulding techniques affects greatly the mechanical behavior [20], compaction technique uses the optimum moisture content which results in closely packed soil, henceforth improved performances [21, 22]. This technique allows to have more closely packed samples by reducing the voids within the samples. Based on previous studies, the optimal activation concentration was investigated by preparing three proportions of the alkali activator 1%, 3% and 5% [23].

In this study, two initial curing temperatures (ICT) were adopted to determine the effect of the ICT variation on the specimen's micro and macro-structural behavior. Previous studies showed the effect of the initial curing temperature and the curing regime on the alkali activation process [24]. Subsequently, the first series was initially cured at 60 °C while the second was initially cured at 105 °C.

The Optimization of curing regime was obtained by subjecting the specimens into different environment. The first series was left unsealed in the laboratory environment at room temperature, contrary to the second series that was sealed inside plastic bags. While the last series was oven dried at 60 °C for the curing period. Three different days, 7, 15 and 90 days, were considered for the curing period. Table 2 summarizes the details of the different set of specimens produced during this investigation. However, some specimens have not been tested without initial curing temperature (ICT) because of their workability. The specimens were losing their shapes as soon as demolded. While they were still wet after 7 days of curing in the laboratory environment (27 °C) without ICT. Thus, they couldn't be handled for mechanical testing as they tend to deform elastically when loaded under compression.

Thus, three (3) curing conditions were tested for the specimens each at two (2) different ICT making six curing tests. Those six curing tests namely are the unsealed room temperature cured specimens (initially cured at ICT1 & ICT2), sealed room temperature cured specimens (initially cured at ICT1 & ICT2) and oven dried specimens (initially cured at ICT1 & ICT2).

2.2. Characterizations

2.2.1. Physical properties

The specific gravity and bulk density of the samples were determined before and after alkali activation to access the effect of the Alkali activation on these properties. Furthermore, the pH for the different specimens under different curing regimes was evaluated to retrieve the effect of the potash on the termite soil at the different percent activation (1%, 3% and 5%) and different curing regime. In addition, the apparent porosity was examined on the activated and non-activated specimens to determine the role of the alkaline activation on the pores. Eq. (2) was used to determine the apparent porosity. The dimensional stability analysis was performed based on the linear shrinkage; it is a way of quantifying the amount of shrinkage likely to be experienced by the material in dry conditions. The analysis was performed with the Eq. (1), it was performed before and after alkali activation to assess the behavior of the specimens under dry conditions, it determines the moisture content below which the material ceases to shrink. It's relevant to the condition of shrinkage due to drying. The dimensional stability was also investigated in wetting conditions by performing the water absorption analysis it's relevant to the condition of the materials' expansion due to wetting and that was performed based on Eq. (3). The analysis allows identifying the behavior of the material when saturated.

$$Ls = 1 - \frac{Ld}{L0} \tag{1}$$

$$AP = 1 - \frac{Bulk\ Density}{Particle\ Density} \tag{2}$$

$$Water\ absorption\ (\%) = \frac{Mwet - Mdry}{Mdry} \times 100 \tag{3}$$
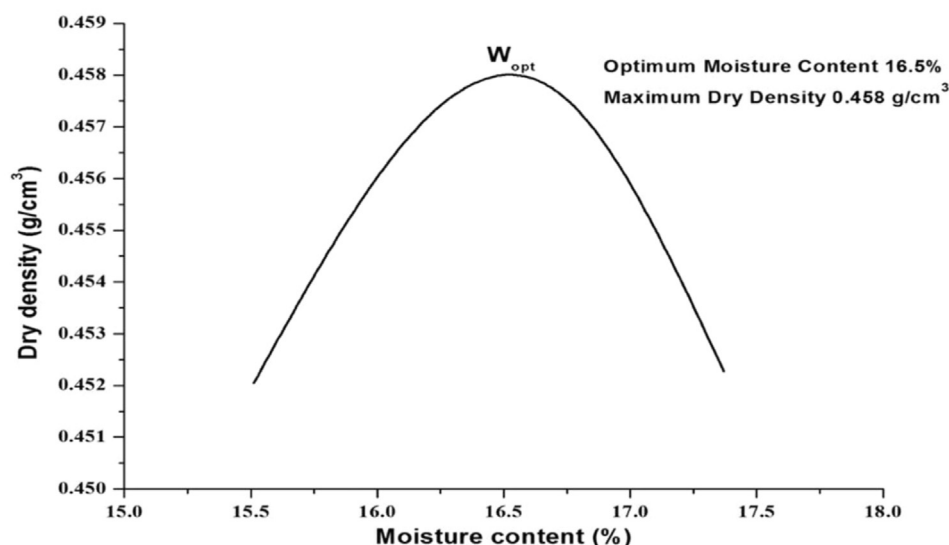
Figure 1. Dry density vs moisture content of termite mound soil.

Table 2. Details of specimen's production.

Designation	Room Temperature				Oven dried	
	RTU1	RTU2	RTS1	RTS2	OD1	OD2
Initial Curing Temperature (°C)	105	60	105	60	105	60
Curing Regime	unsealed	unsealed	sealed	sealed	60	60

2.2.2. X-ray diffraction (XRD) analysis

To determine the different minerals in the specimens and their respective transformations, X-ray Diffraction (XRD) was performed on the specimens after 15 days. The analysis was achieved using an X-ray Diffractometer model ARL'XTRA (Thermo Scientific, Switzerland) with range of 10–70° (2θ) at 0.02° 2θ steps integrated at the rate of 4.0s per step. The patterns were processed using Match Software.

2.2.3. Microstructure observation

The morphology and microstructure of the termite's soil (TS) and alkali activated termite's soil (AATS) were examined with the aid of Scanning Electron Microscopy-Energy Dispersive Spectroscopy (SEM-EDX) to examine the repercussions of the chemical stabilization on the microstructure and morphology of the TS. Thus, the analysis was carried for all the specimens. The analysis was carried in a Carl Zeiss Model EVO LS10 instrumented with an EDX system that can detect elements between Sodium and Uranium. Prior to the analysis the specimens were coated with gold, to ease the imaging of the specimen's superficial appearances.

2.2.4. Fourier Transform Infra-Red (FTIR) spectroscopy

To examine the type of bonds existing between the different elements of the Termite Soil (TS) and the Alkali Activated Termite Soil (AATS), Fourier Transform Infra-Red (FTIR) was carried on the different specimens. The analysis was conducted with a Thermo Scientific Nicolet iS5 FTIR system (Thermo Scientific, USA). The powder form of the different specimen was mixed with Potassium Bromate (KBr) in a ratio of 5:1 separately for each specimen. The software Know it all Bio-Rad was used to analyze the data obtained.

2.2.5. Mechanical properties

The mechanical properties examined was the uniaxial compression strength carried on a Universal testing machine Model 4002 & UTM7001 (Utest, Ankara, Turkey) at a loading rate of 0.6 kN/s. The specimens were tested after 7, 15 and 90 days for all the sets of specimens. The specimens from the different curing modes were oven dry for 24 h before testing. The compressive strengths were obtained from Eq. (4), prior to the testing the real dimensions of the specimens were estimated using Vernier calipers.

$$\sigma c = \frac{Fi}{Ai} \tag{4}$$

Where σc is the compressive strength in MPa, F_i is the applied load in N, and A_i is the cross-sectional area in mm^2. During loading the specimens deformed and failed differently hence the deformed specimens were analyzed with SEM to understand the bonds breakage. The software Origin was used to analyze the data and determine the different variations observed in the mechanical behavior.

3. Results and discussions

3.1. From microstructural to macroscopic behavior

#### 3.1.1. Macroscopic behavior

The micro and macro-structural behavior of construction materials affects greatly their properties, therefore it's important to link the two from the SEM to Photo images. Photos of the different sets of specimens were taken directly after demolding as shown in Figure 2. The specimens initially cured at 105 °C expanded beyond the mould, however that
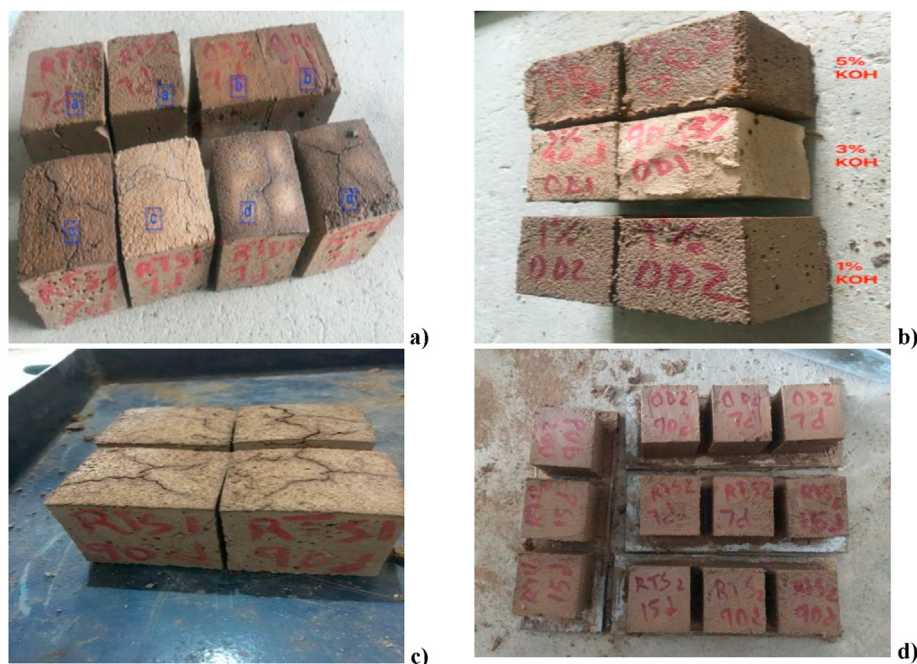
Figure 2. a) Specimen with different curing regime at 3% of potash, b) Different percent of the activator: 1%, 3% and 5%, c) Noticeable cracks observed for the samples initially cured, d) Smooth surface exhibited by specimens initially cured at 60°C.
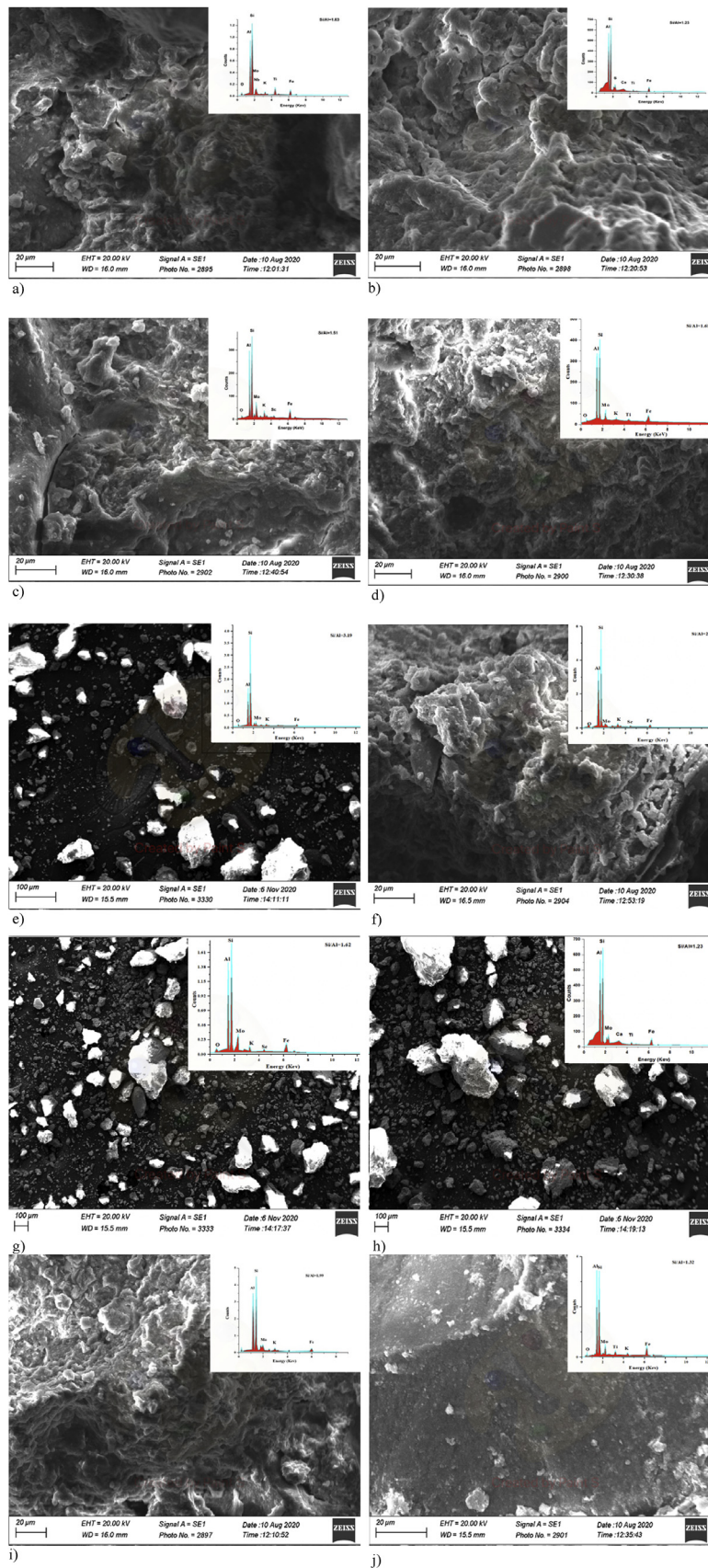
Figure 3. Morphology of different specimens with chemical content micrographs of a) RTU1 b) RTU2, c) OD2, d) OD1 at 3wt% of potash. Of specimens with 1wt%: e) RTU2, f) RTS2, g) OD2 and specimens with 5wt% h) RTU2, i) RTS2 and j) OD2. With RT: Room Temperature curing, OD: Oven- Dried curing, U: Unsealed specimens, S: Sealed specimens,1: Initial curing temperature of 105°C, 2: Initial curing temperature of 60°C.
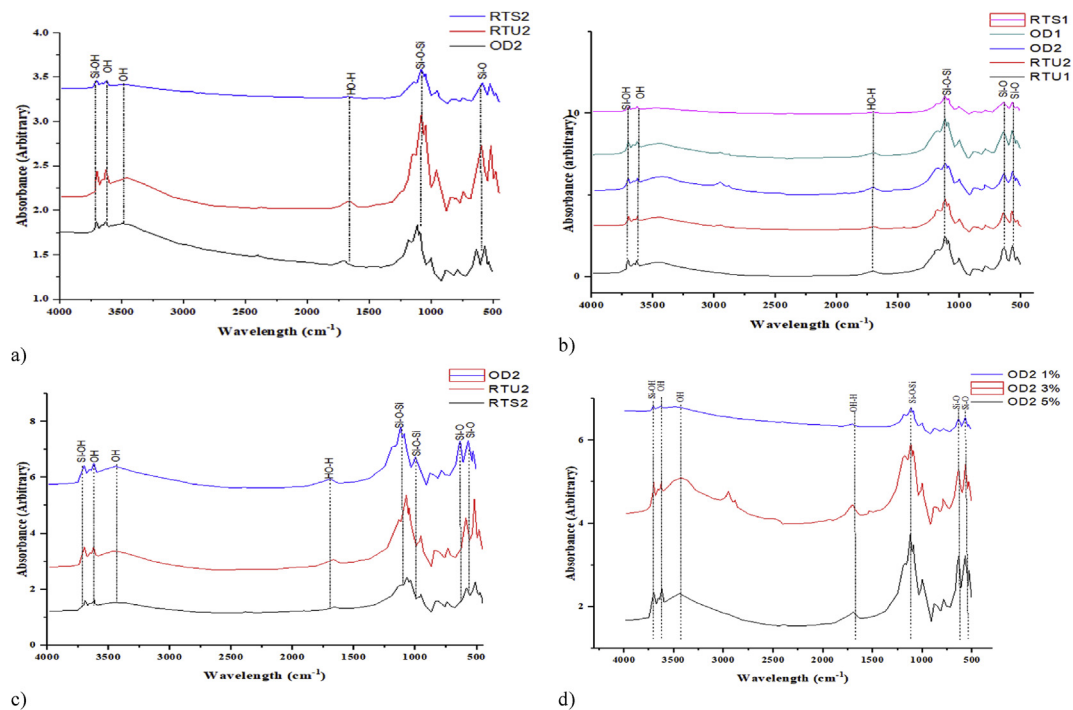
Figure 4. FTIR pattern for: a) specimens with 1wt% Potash, b) specimens with 3wt% Potash, c) specimens with 5wt% Potash and d) specimens at optimum curing regime for all the activation level.

expansion wasn't considerable. The remaining specimens didn't show any noticeable shrinkage or expansion. Figure 2 b shows the difference in color that was very noticeable with the variation of activation level; at 1wt% of potash the specimens were dark in complexion while they are lighter at 3wt% but they become darker when the activator increased to 5wt%. The effect of the curing regime was considerable in terms of the sealing; the specimens that were sealed exhibited smooth surface with no cracks (Figure 2 d) but were still wet at 15 days contrary to the unsealed specimens which exhibited significant surface cracks in Figure 2 a. However, specimens initially cured at higher temperature (105 °C) presented remarkable surface cracks while specimens initially cured at low temperature displayed smooth surface (60 °C) as shown in Figure 2 c&d indicating the effect of the ICT on the crack's initiation.

3.1.2. Microstructural examination

The SEM images show that the specimens cured at high temperature RTU1 (Figure 3 a) presented some surface cracks and pores (Figure 3 e) which are generated by the shrinkage during the curing process. A possible explanation is that the reaction rate is slow as it can be seen from the low Si/Al ratio displayed by the specimens during the curing process. A flocculation within the particles was triggered by the activator resulting in shrinkage cracks around the external surface of the specimens. Meanwhile, the specimens with greater Si/Al = 1.91 exhibited more spherulitic new phases filling the pore spaces by binding the particles as shown in Figure 3 b indicating the transformation of the matrix from irregular shapes to spherulitic. In addition to the difference in Si/Al ratio, slight compositional differences were noticed between the specimens. The same phenomenon was reported by Slaty et al. in the alkaline activation of kaolinitic clay with NaOH [25]. The relict cracks detected in Figure 3 f can be the result of the unreacted termite soil indicating a lower dissolution rate of the termite soil and potash. Trace of iron oxide phases present in the EDX results could possibly play a role in the color change after curing of the specimens at high temperature (105 °C) as perceived in the macroscopic observations in Figure 2. The Si/Al ratio

varied from 2.29 to 3.19 for the specimens containing 1wt% of activator, while the Si/Al ratio varied from 1.23 to 1.63 and 1.32 to 1.99 for 3wt% and 5wt% potash respectively. That reveals the insignificant contribution in Silicon and Aluminum content by the potash activator. In all cases, the specimens initially cured at high temperature displayed higher Si/Al ratio in the 4 curing regimes contrary to the sealed specimens where the highest Si/Al ratio was displayed by the initially low temperature cured specimens. This can be explained by the composition and chemical reactions taking place within the sealed environment. Criado et al. (2008) observed that this parameter played an essential role in the kinetics, the structure and the composition of the initial gel formed [26] thus the mechanical behavior noticed.

3.1.3. Molecular bonding (FTIR)

Figure 4 shows the results of the FTIR analyses performed on all the specimens at 15 days. Sharp Peaks attributed to Si–OH were located at 3619 cm^{-1} to 3695 cm^{-1} for all the specimens with the exception of RTU2 and RTS2 at 1wt%. In these specimens the formation of new peaks was observed at 3854 cm^{-1} attributed to the Si–OH revealing the significant displacement of the band. Broad peaks assigned to the stretching –OH were observed around 3430 cm^{-1} in all the specimens with a band shift reaching values of ±20 cm^{-1}, shift values are characteristic of aluminosilicate network formation [27]. Contrary to the specimens OD2 at 1wt% in which higher wavenumbers was evidenced around 3850 cm^{-1} and 3479 cm^{-1}. In any case, all the specimens presented broad peaks attributed to bending H–O–H around 1650 cm^{-1} with very slight shift values ranging ±15 cm^{-1}. The main peaks located around 1090 and 500 cm^{-1} characterize the silicate structure with the assigned vibration of Si/Al–O and S–S stretching bond respectively reflecting the formation of amorphous aluminosilicate gel [28]. For the different curing regimes, the displacement of the different vibrations group is very imperceptible (Figure 4 a–c), whereas the change in intensity is remarkable for the different activation level (Figure 4 d). At 1wt% activator the FTIR spectrum is dominated by 1035cm^{-1} assigned to the vibration of Si/Al–O but
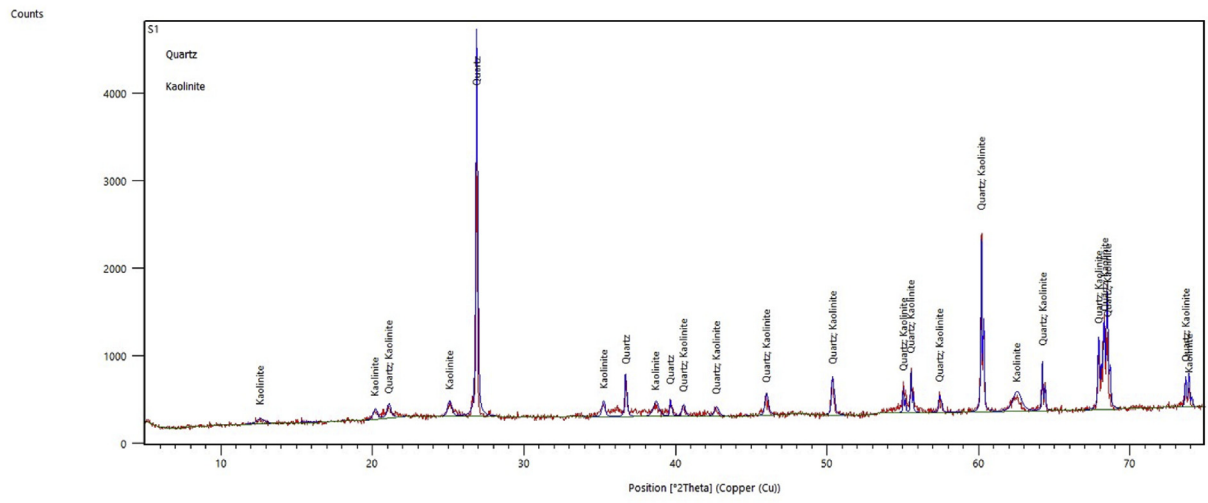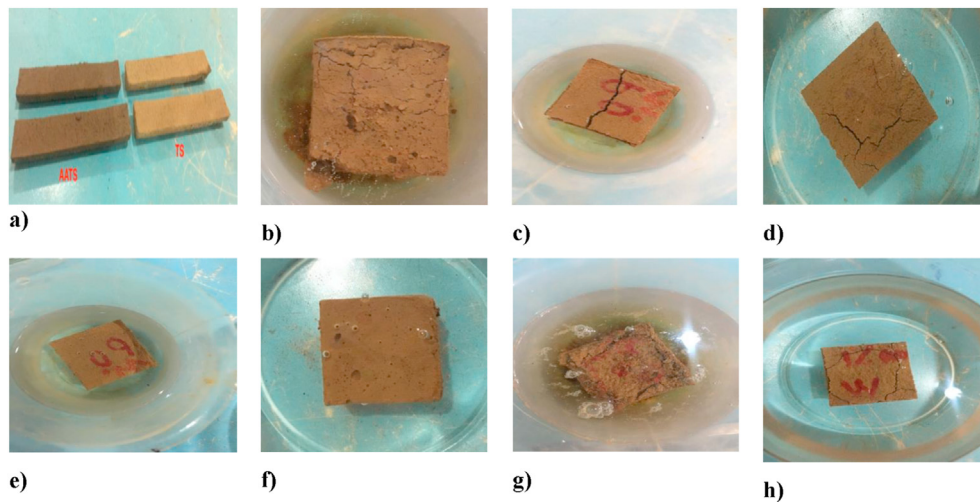
a)
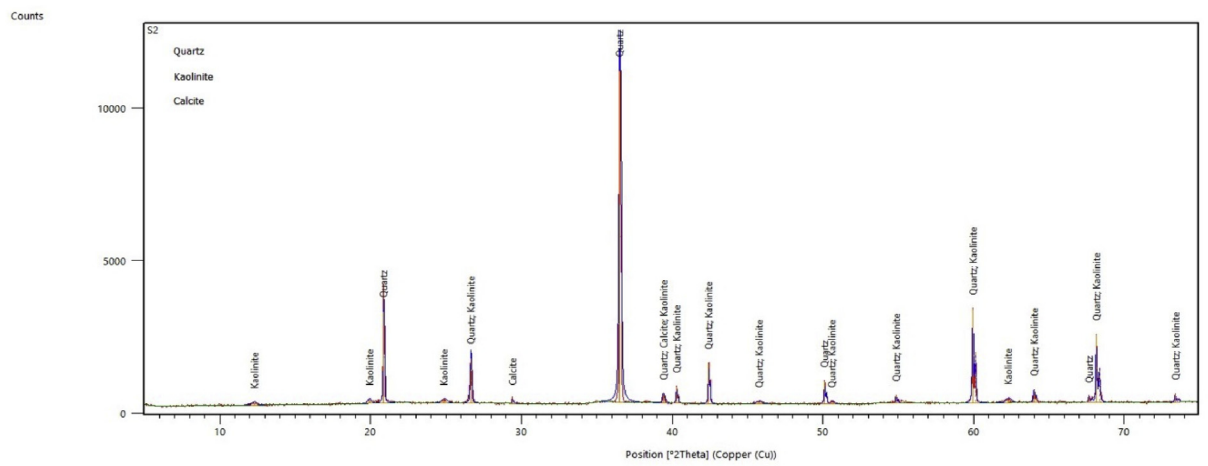
b)
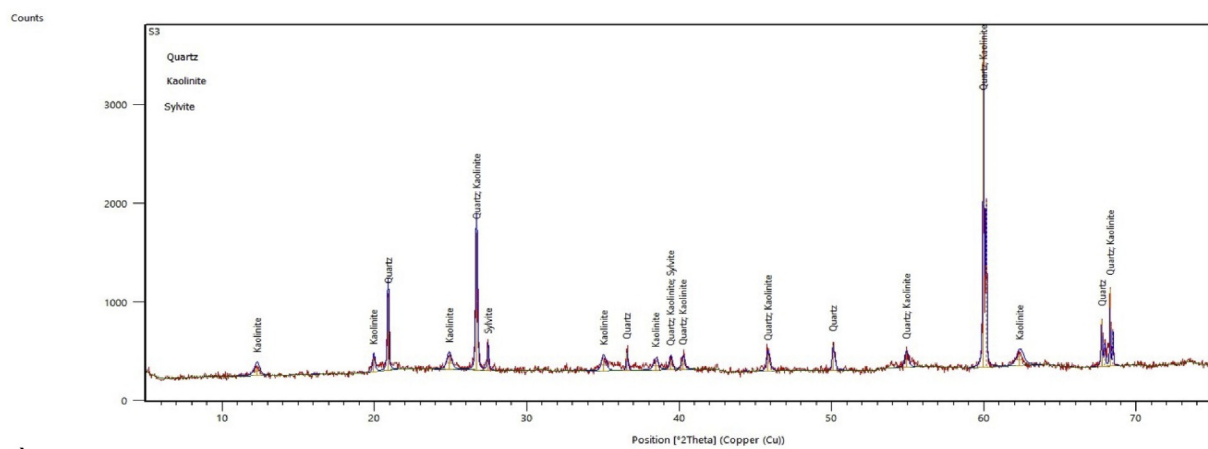
c)

Figure 5. XRD patterns for Alkali Activated Termite's Soil (AATS) at: a) 1wt% activator, b) 3wt% activator and c) 5wt% activator.

Figure 6. a) Linear shrinkage of TS and AATS, b) saturated RTU1 specimens, c) saturated RTU2 specimens. d) saturated OD1 specimens. e) saturated OD2 specimens, f) saturated RTS1 specimens, g) specimens activated at 5% Alum, h) specimens activated at 1% Alum. With RT: Room Temperature curing, OD: Oven- Dried curing, U: Unsealed specimens, S: Sealed specimens,1: Initial curing temperature of 105 °C, 2: Initial curing temperature of 60 °C.
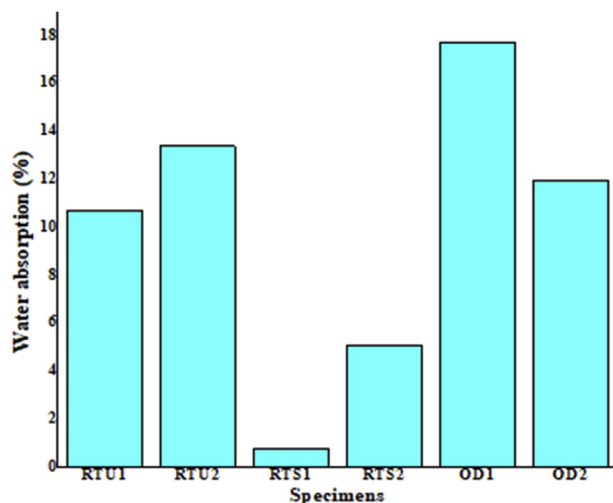
Figure 7. Water absorption of the specimens under different curing regime.

with weaker intensity than in the specimens with 3wt% and 5wt%. However, 3wt% the peaks assigned to the stretching –OH were intense around 3430 cm^{-1} and the band assigned to the vibration of Si/Al–O reveal the formation of bond by the ring vibration of Si–O [28].

3.1.4. Transformation of present minerals (XRD)

XRD patterns of the AATS for the different activation level are presented in Figure 5, they represent the different transformation undergone by the minerals. The diffraction patterns showed that there is an appreciable transformation of the AATS with different activation level. The crystalline phases detected around 2Θ = 21.5° and 2Θ = 26.5° were

transformed from quartz-kaolin to kaolin and from quartz to quartz-kaolin respectively from 1wt% to 3wt% and 5wt% potash.

At 3wt% of potash, Calcite (CaCO$_3$) [29] was detected at 2Θ = 29.5° while it was inexistant at 1wt% of potash (Figure 5 a &b), meanwhile the formation of Sylvite (KCl) [30] was observed for 5wt% potash around 2Θ = 27.5°(Figure 5 c). In any case, at 1wt% activation the crystalline phases are mainly quartz and kaolin while at 3wt% quartz and kaolin peaks showed higher intensity than other activation levels, this reveals the higher dissolution reactivity of the termite soil precursor in the alkaline environment at that level. Additionally, formation of Calcite at 3wt% was observed then it was transformed into Sylvite at 5wt% activation. These phases transformation can be attributed to the potassium induction made by the activator and the formation of gel. The formation of calcite is related to the rapid dissolving of Ca obtained in the precursor in the alkaline solution and the precipitation of Ca(OH)$_2$ finally transforming into calcite [29]. While the formation of sylvite can be explained by the sulfate dependent oxidation taking place during the alkali activation of termite's soil [31]. Both calcite and sylvite are evaporite minerals. Thus, some of the quartz and kaolin remained unaltered during the activation revealing lower dissolution reaction between the remained quartz and kaolin with the activator. But calcite exhibits retrograde solubility (it becomes less soluble in water as the temperature increases) [32].

3.1.5. Dimensional stability of the Alkali activated Termite's soil (AATS)

The linear shrinkage presented in Figure 6 a illustrates the behavior of the TS and AATS for the specimens. It was noticed that the shrinkage of both the TS and AATS were not really considerable in spite that the AATS showed less shrinkage. A possible explanation is that the alkaline reaction has induced some flocculation among the particles confirming the microstructural observations. Prud'homme et al. (2010) showed that the oxidation of silica during the alkali activation may produce hydrogen gas [33] inducing particles flocculation. That same reaction may have generated more pores within the specimens. Thereby, the specimens cured initially at low temperature under room temperature showed less

Table 3. Influences of the alkaline activation on the physical properties.

Physical Properties/Specimens	Linear Shrinkage (%)	Bulk Density (g/cm^3)	Apparent porosity (%)	Specific gravity
*TS	6.7	1.47	41.9	2.61
[1]AATS	4.8	1.49	43.5	2.69

* TS: termite soil.
[1] AATS: Alkali Activated Termite's soil.
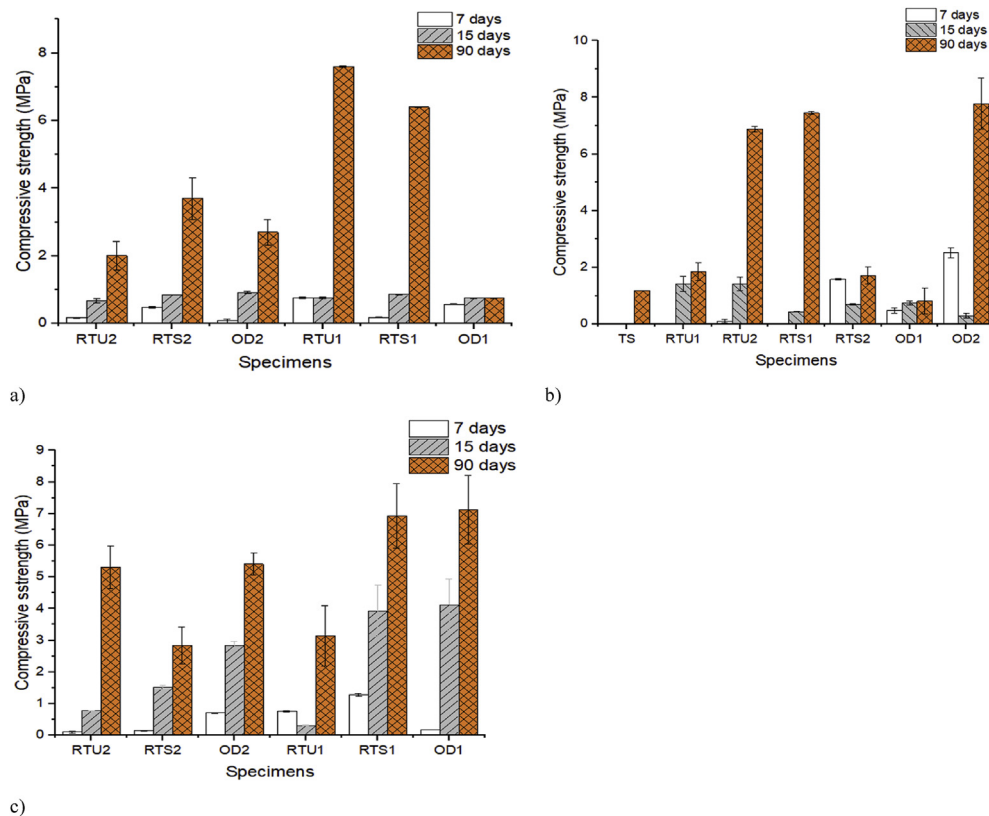
Figure 8. Compressive strength at 7,15 and 90 days for: a) 1wt% activation, b) 3wt% activation, c) 5wt% activation with RT: Room Temperature curing, OD: Oven-Dried curing, U: Unsealed specimens, S: Sealed specimens,1: Initial curing temperature of 105°C, 2: Initial curing temperature of 60°C.

sensitivity to water (Figure 6 c) compared to oven dried (Figure 6 d and d) this is in accordance with the shrinkage mechanism investigated by Hailong Ye [34]. Ye et al. have established the correlation between the Relative Humidity and Shrinkage, as the viscous deformations occurring at high Relative Humidity triggered by the rearrangement of particles [35] contributes to the general shrinkage [34, 35]. In our study, the specimens initially cured at high temperature showed more sensitivity to water (Figure 6 b).

The effect of the alkaline activation on the water absorbability of the specimens are summarized in Figure 7 a. Sealed, and room temperature cured specimens showed lower water absorption rate revealing more dense specimens. Figure 7 b. shows the effect of the Alkaline activation on some physical properties (bulk density, specific gravity and apparent porosity). While the Table 3 present a comparism of the physical properties between the termite soil and alkali activated termite soil.

3.1.6. Influences of the alkaline activation on the soil's pH

The pH is a useful indicator of the AATS behaviour. The most critical role of the alkaline activator in an alkali-activated material is to dissolve the aluminosilicate and accelerate the reaction, which is obtained by generating a high pH [26]. Additionally, the effect of the pH on the activation of the TS is highly dependent upon the potash composition, since the solubility of silica and alumina increases causing the silicate to develop a greater mechanical strength. The alkaline nature of the potash affects the pH of the TS by increasing it or decreasing it depending on the ICT and curing regime. The consumption of alkalinity indicates that the formation of bonds and strengthening of the TS are occurring. The variation of the pH was slightly significant for the specimens with the same activator content for all curing regimes. That indicates that the curing regime affects the pH at a very insignificant level for the AATS. However, specimens initially cured at lower temperature displayed higher pH revealing the effect of the ICT on the specimen's alkalinity. Consequently, the potash reacted with the TS particles to cause the soil

particles to flocculate into finer grain (as observed earlier in the SEM micrographs) or coarser grains [25]. When there are no significant reactions taking place between the activator and the soil that suggest that the soil remained intact.

3.1.7. Mechanical behavior of the AATS

The compressive strength of all the specimens at the age of 7, 15 and 90 days for the different activation levels and different curing regimes are presented in Figure 8. From the compressive strength results it can be noticed that at the early age of 7 days the specimens cured at lower temperature presented higher compressive strength than specimens initially cured at high temperature. The same trend was observed for the age of 15 days with exception of the specimens that were oven-cured at 60 °C revealing the optimum initial curing temperature for the AATS. During testing the specimens failed by formation of oblique cracks which grew until separation of the specimens into 2 or more pieces. However, the innermost part of the specimens was less subjected to the deformation and it resisted until critical loading before failing. A possible explanation is that during the curing process, the existing calcite experienced a regressive solubility [36] due to the effect of curing temperature. The compressive strength has increased as the temperature increased. In any case, the highest compressive strength was attained by the specimens containing 3wt% activator under oven-dry regime revealing the optimum activation percent. Long curing times give origin to the formation of silica-rich products [26], allowing satisfactory formation of the potassium aluminosilicate gel. Henceforth, favoring the development of the material's final resistances. The material owes its good mechanical performance primarily to the sodium aluminosilicate gel [37]. The standard deviation is so high in some cases because of the significant variation among the set of specimens tested for the compressive strength. Meanwhile, it is low for the sets where the variations among the specimens tested is not very significant (low), but the two closest results out of the tree have been considered to remediate to the high standard deviation.

4. Conclusions

The propitious experimental results obtained from this investigation can be used to produce AATS for sustainable and eco-friendly masonry units. Indeed, alkaline activation is a key component technique for a green and sustainable global future in construction materials. This article reported the special effect of the activation concentration, initial curing temperature and curing regimes on the elemental, micro- and macro-structural behavior of AATS. The main findings of the study are summarized as follows:

- The alkaline activation favored reduction of linear shrinkage of the specimens. As the activation concentration increases, the linear shrinkage of the AATS decreases.
- The optimum ICT was 60 °C as it favored dimensional stability by improving water sensitivity in dry and wet conditions. Also, by the impressive mechanical behavior displayed by the specimens initially cured at that low temperature. Although, the dissolution of alumina and silica from natural aluminosilicates require higher temperature.
- From the microstructural, elemental and compositional analyses, it can be concluded that the formation of phases is engendered by the dissolution of the potash. Thus, these phases are probably K-aluminosilicate gels responsible for the observed bindings.
- The ideal activation concentration for the compressive strength is 3wt %. In any case, the compressive strength does not increase proportionally with the activator concentration, whereas the highest compressive was obtained for 3wt% of the Potash.
- The highest compressive strength attained by the AATS in this study is 7.79MPa which is higher than the minimum required compressive strength by the ASTM C129 for nonload-bearing masonry units is (3.45 MPa) [38]. Therefore, a potential application of the AATS in construction is non load-bearing masonry units.

Considering the availability of aluminosilicate globally and termite mound soil in the sub-Saharan region particularly, this study shows that the alkaline activation can be an environmental-friendly technique to process the termite mound soil into a valuable construction material. Consequently, the results will contribute to develop sustainable materials in construction from waste (the termite soil is considered as waste). The results are valuable for Sub-Saharan and regions where the high energy embodied materials are not affordable and where those natural materials are available (termite soil). The development of that technology represents an important opportunity to transform the natural waste into valuable, renewable and sustainable construction materials to preserve the ecosystem from greenhouses gas emission. The future implications of this investigation will be the reduction of cement utilization in construction resulting in preserving the ecosystem, reducing housing prices in region with limited means, promoting and engineering local materials. For future work, the termite mound soil can be subjected to pre-heat treatment before its activation to obtain more improved mechanical behavior.

Declarations

Author contribution statement

Assia Aboubakar Mahamat: Conceived and designed the experiments; Performed the experiments; Analyzed and interpreted the data; Contributed reagents, materials, analysis tools or data; Wrote the paper.

Ifeyinwa Ijeoma Obianyo, Olugbenga Ayeni, Salifu T. Azeko: Analyzed and interpreted the data.

Blasuis Ngayakamo, Numfor Linda Bih: Performed the experiments.

Holmer Savastano Jr: Conceived and designed the experiments; Analyzed and interpreted the data.

Data availability statement

Data will be made available on request.

Declaration of interests statement

The authors declare no conflict of interest.

Additional information

No additional information is available for this paper.

References

[1] N.Y. Jadhav, Green energy and technology green and smart buildings advanced technology options [Online]. Available: http://www.springer.com/series/8059.

[2] N. Afeez, S.A. Adeshina, A. Inci, M.M. Boukar, A framework for Poultry weather control with IoT in sub-Saharan Africa, in: 15th International Conference on Electronics, Computer and Computation (ICECCO), IEEE, 2019, p. 2019.

[3] United Nations Statistics Division (UNSD) and Division of the Department of Economic and Social Affairs (DESA)., "Make cities and human settlements inclusive, safe, resilient and sustainable." Accessed: Nov. 06, 2020. [Online]. Available: https://unstats.un.org/sdgs/report/2019/goal-11/.

[4] R.K. Kandasami, R.M. Borges, T.G. Murthy, Effect of biocementation on the strength and stability of termite mounds, Environ. Geotech. 3 (2) (Apr. 2016) 99–113.

[5] M. L, B.V.P. Jouquet, jouquet2002, Insectes Soc. 49 (2002) 1–7.

[6] D.E. Pomeroy, This Content Downloaded from 128.184.220.23 on Fri, 1978 [Online]. Available: http://www.jstor.orgURL:http://www.jstor.org/stable/2402920http://www.jstor.org/page/info/about/policies/terms.jsp.

[7] I.L. Ackerman, W.G. Teixeira, S.J. Riha, J. Lehmann, E.C.M. Fernandes, The impact of mound-building termites on surface soil properties in a secondary forest of Central Amazonia, Appl. Soil Ecol. 37 (3) (Nov. 2007) 267–276.

[8] M.K. Idris, M.M. Boukar, S.A. Adeshina, Analysis of Bad Roads Using Smart Phone, Dec. 2019.

[9] B. Jean-Pierre, et al., Spatial distribution and Density of termite mounds in a protected habitat in the south of Cote d'Ivoire: case of national floristic center (CNF) of UFHB of Abidjan, Eur. Sci. J. 11 (3) (2015).

[10] A.U. Elinwa, Experimental characterization of Portland cement-calcined soldier-ant mound clay cement mortar and concrete, Construct. Build. Mater. 20 (9) (Nov. 2006) 754–760.

[11] B.A. Akinyemi, A. Bamidele, A. Oluwanifemi, Influence of water repellent chemical additive and different curing regimes on dimensional stability and strength of earth bricks from termite mound-clay, Heliyon 5 (2019), e01182.

[12] R.M. Gandia, A.A.R. Corrèa, F.C. Gomes, D.B. Marin, L.S. Santana, "Physical, mechanical and thermal behavior of adobe stabilized with 'synthetic termite saliva, Eng. Agric. 39 (2) (Mar. 2019) 139–149.

[13] R.K. Dhir, G.S. Ghataora, C.J. Lynn, Geotechnical applications, in: Sustainable Construction Materials, Elsevier, 2017, pp. 185–207.

[14] J.L. Provis, Alkali-activated materials, in: Cement and Concrete Research, 114, Elsevier Ltd, Dec. 01, 2018, pp. 40–48.

[15] J.L. Provis, J.S.J. van Deventer, RILEM state-of-the-art reports state-of-the-art report, RILEM TC 224-AAM [Online]. Available: http://www.springer.com/series/8780.

[16] B.C. McLellan, R.P. Williams, J. Lay, A. van Riessen, G.D. Corder, Costs and carbon emissions for geopolymer pastes in comparison to ordinary portland cement, J. Clean. Prod. 19 (9–10) (Jun. 2011) 1080–1090.

[17] P.N. Lemougna, U.F.C. Melo, E. Kamseu, A.B. Tchamba, Laterite based stabilized products for sustainable building applications in tropical countries: review and prospects for the case of Cameroon, Sustainability 3 (1) (Jan. 2011) 293–305.

[18] Hans Kuhl, Slag Cement and Process of Making the Same, United States patent office," New York, Oct. 1908.

[19] M. Falah, R. Obenaus-Emler, P. Kinnunen, M. Illikainen, Effects of activator properties and curing conditions on alkali-activation of low-alumina mine tailings, Waste Biomass Valorization 11 (9) (Sep. 2020) 5027–5039.

[20] E.B. Ojo, K. Mustapha, R.S. Teixeira, H. Savastano, Development of unfired earthen building materials using muscovite rich soils and alkali activators, Case Stud. Construct. Mater. 11 (Dec) (2019).

[21] Q.B. Bui, J.C. Morel, S. Hans, P. Walker, Effect of moisture content on the mechanical characteristics of rammed earth, Construct. Build. Mater. 54 (Mar. 2014) 163–169.

[22] A. W. Bruno, D. Gallipoli, C. Perlot, and J. Mendes, "Effect of very high compaction pressures on the physical and mechanical properties of earthen materials," *E3S Web of Conferencese3sconf/20160914004*.

[23] L. Reig, L. Soriano, M.v. Borrachero, J. Monzó, J. Payá, Influence of the activator concentration and calcium hydroxide addition on the properties of alkali-activated porcelain stoneware, Construct. Build. Mater. 63 (Jul. 2014) 214–222.

[24] S. Ahmari, L. Zhang, J. Zhang, Effects of activator type/concentration and curing temperature on alkali-activated binder based on copper mine tailings, J. Mater. Sci. 47 (16) (Aug. 2012) 5933–5945.

[25] F. Slaty, H. Khoury, J. Wastiels, H. Rahier, Characterization of alkali activated kaolinitic clay, Appl. Clay Sci. 75 (76) (May 2013) 120–125.

[26] M. Criado, A. Fernández-Jiménez, A.G. de la Torre, M.A.G. Aranda, A. Palomo, An XRD study of the effect of the SiO_2/Na_2O ratio on the alkali activation of fly ash, Cement Concr. Res. 37 (5) (May 2007) 671–679.

[27] Claudio Finocchiaro, Germana Barone, Paolo Mazzoleni, Cristina Leonelli, Ameni Gharzouni, Sylvie Rossignol, FT-IR study of early stages of alkali activated materials based on pyroclastic deposits (Mt. Etna, Sicily, Italy) using two different alkaline solutions, Construct. Build. Mater. 262 (November 2020) 120095.

[28] L.N. Tchadjié, et al., Potential of using granite waste as raw material for geopolymer synthesis, Ceram. Int. 42 (2) (2016) 3046–3055.

[29] P.T. Staudigel, P.K. Swart, Isotopic behavior during the aragonite-calcite transition: implications for sample preparation and proxy interpretation, Chem. Geol. 442 (Nov. 2016) 130–138.

[30] S.M. MacKenzie, J.W. Barnes, Compositional similarities and distinctions between titan's evaporitic terrains, Astrophys. J. 821 (1) (Apr. 2016) 17.

[31] G.B.P.M. Claudio Finocchiaroa, FT-IR study of early stages of alkali activated materials based on pyroclastic deposits (Mt. Etna, Sicily, Italy) using two different alkaline solutions, Construct. Build. Mater. 262 (2020).

[32] J.W. Morse, R.S. Arvidson, A. Lüttge, Calcium carbonate formation and dissolution, Chem. Rev. 107 (2) (Feb. 2007) 342–381.

[33] E. Prud'homme, et al., Silica fume as porogent agent in geo-materials at low temperature, J. Eur. Ceram. Soc. 30 (7) (May 2010) 1641–1648.

[34] H. Ye, C. Cartwright, F. Rajabipour, A. Radlińska, Understanding the drying shrinkage performance of alkali-activated slag mortars, Cement Concr. Compos. 76 (Feb. 2017) 13–24.

[35] H. Ye, A. Radlińska, Shrinkage mechanisms of alkali-activated slag, Cement Concr. Res. 88 (Oct. 2016) 126–135.

[36] H. Drake, et al., Extreme 13 C depletion of carbonates formed during oxidation of biogenic methane in fractured granite, Nat. Commun. 6 (May 2015).

[37] M. Torres-Carrasco, F. Puertas, Alkaline activation of different aluminosilicates as an alternative to Portland cement: alkali activated cements or geopolymers La activación alcalina de diferentes aluminosilicatos como una alternativa al Cemento Portland: cementos activados alcalinamente o geopolímeros, 2017 [Online]. Available: www.ricuc.cl.

[38] American Society for Testing Materials C129, Non load-bearing Masonry, "ASTM C129." Accessed: Mar. 06, 2020. [Online]. Available: https://www.astm.org/Standards/D854.